20101103A

別添１

厚生労働科学研究費補助金

医療機器開発推進　研究事業

細胞特異的・高効率なsiRNA送達法の開発と難治性肝疾患治療への展開

平成２２年度　総括研究報告書

研究代表者　川上　茂

平成23（2011）年　5月

目　　次

厚生労働科学研究費補助金（医療機器開発　研究事業）
（総括）研究報告書

細胞特異的・高効率なsiRNA送達法の開発と難治性肝疾患治療への展開

研究代表者　川上　茂　京都大学大学院薬学研究科　講師

研究要旨：本研究では、細胞特異的・高効率なsiRNA送達法を開発し、難治性肝疾患治療への応用を目指す。今年度は、肝類洞血管内皮細胞指向性を有する超音波応答性マンノース修飾バブルリポソームを用いたsiRNAデリバリーによる肝炎治療法構築が目標である。超音波応答型マンノース修飾バブルリポソーム製剤を用いて、好中球の血管外遊走の後期に関与する細胞間接着因子(ICAM-1) に対するsiRNAとの複合体を調製法とその体内動態特性やLPS誘発性肝炎モデルマウスに対する薬理効果の評価を行った。その結果、超音波応答型マンノース修飾バブルリポソーム製剤を用いることで、ICAM-1 siRNAが肝類洞血管内皮細胞やKupffer細胞などの肝臓非実質細胞へ選択的に送達され、LPS誘発性肝障害モデルマウスにおいて、有意な抗炎症効果を発揮することが確認された。

A．研究目的

核酸の高効率なin vivo送達は、小動物を用いて原発臓器・細胞を対象とした遺伝子機能解析並びに病態モデル動物作成による創薬標的遺伝子/タンパク質および治療薬探索や直接作用を発揮させる遺伝子治療を通じて、創薬のためのライフサイエンス研究の進展に貢献する。その実現のためには、標的細胞に核酸医薬を送達する技術の開発が不可欠であり、現在、世界中でベクター開発が活発に行われている。とりわけ近年、siRNAを用いた標的指向DDS送達による治療効果に関する報告がなされ、今後の医療展開が期待されている。

リポソームや高分子など非ウイルスベクターによる送達は、低免疫原性、安全性、調製の容易さから広範囲な研究施設での使用やヒト適用において利点を有する。申請者らは、肝臓を構成する各細胞が固有に有し、厳密な基質認識性を有する糖鎖認識機構に認識されるように分子設計した糖修飾カチオン性リポソームを開発した。その後、全身・臓器・細胞レベルでの定量的な動態解析・最適化を行い、細胞選択的な核酸医薬送達並びに治療展開に成功した。また、糖修飾リポプレックスとバブルリポソームの併用と超音波(ultrasound; US)照射により標的細胞での細胞穿孔に基づいた遺伝子発現の増強に成功した。

このような背景を基盤として本研究では、申請者らが開発を進めている糖鎖による生体分子の特異的認識に基づくin vivo誘導と超音波による細胞穿孔を組み合わせた新規DDS技術を、創薬シーズが多く生体での多様な作用が期待できるsiRNA送達法に応用し開発を進める。さらに、肝類洞血管内皮並びに肝星（伊東）細胞を標的とした高効率送達による難治性肝疾患に対する新規治療法開発を目指す。

1年目は、超音波応答性マンノース修飾バブルリポソーム(Man-$PEG_{2,000}$ bubble liposome) の調製法と体外からの超音波照射による肝類洞血管内皮への細胞特異的・高効率なsiRNAの送達法の開発と肝炎治療への応用が目標である。

B．研究方法

当初の1年目の研究計画では、ICAM-1に対するsiRNAを用いてマウス肝類洞血管内皮細胞を標的としたナノメディシンの設計及び肝炎へのDDS戦略を行う予定であった。DDS製剤としては、マンノース修飾バブルリポソーム (Man-$PEG_{2,000}$ bubble liposome) を用い、未修飾バブルリポソーム (Bare-$PEG_{2,000}$ bubble liposome) を対照として評価した。脂質組成としては、我々のプラスミドDNAを用いた以前の報告（Biomaterials, 31 (30), 7813-7826 (2010)）で示すように、DSTAP: DSPC: Man-$PEG_{2,000}$-DSPEをモル比で7:2:1の割合で混合したものを用い、リポソームを調製後、パーフルオロプロパンガスを封入した。

ζ電位、平均粒子径などの物理化学的性質は、ゼータサイザーナノ（マルバーン社製）により評価をおこなった。また、LPS/D-ガラクトサミンの腹腔内投与によりLPS誘発性肝炎モデルマウスを作成し、10 μg siRNA/マウス（C57BL/6系雄性マウス、17－19 g）の投与量で尾静脈より投与し、5 分後にマウス腹腔側から直径20 mmのプローブを用いて超音波(US) 照射（frequency 1.045 MHz; duty 50%; burst rate 10 Hz; intensity 4.0 W/cm^2; sonopore-4000 sonicator, ネッパジーン社製）を 2 分間行った。

肝臓中ICAM1発現の評価は、ELISA法と定量的PCR法により行った。炎症性サイトカインとしては、血清TNFα, IFNγ, IL-6濃度をELISA法により評価した。肝毒性に関しては、血清ALT, AST濃度を測定した。また、肝組織切片を作成し顕微鏡での観察を行った。siRNA (21 mer) はジーンデザイン社より購入し、配列の最適化検討を行った結果、最終的には、

以下の配列を有するものを用いた。5'-GAA AGA UCA GGA UAU ACA AdTdT-3'(センス鎖)、5'-UUG UAU AUC CUG AUC UUU CdTdT-3' (アンチセンス鎖)。対照のscramble siRNAとしては、以下のものを用いた。5'-GUA CUG UAC CAC UCU CAA AdTdT-3'(センス鎖)、5'-CUG UUC CGC AUU UUA AUU UdTdT-3' (アンチセンス鎖)。

蛍光標識は、alexa-488を用い、本DDS製剤を投与 1 時間後にコラゲナーゼ灌流法により肝臓実質細胞と肝臓非実質細胞を分離し、さらに肝臓非実質細胞に関しては、磁気細胞分離法により肝類洞血管内皮細胞とKupffer細胞を分離した。

(倫理面への配慮)

動物実験を行うにあたり、京都大学で策定された動物実験倫理規定に従ってプロトコルを作成し、倫理委員会によって承認を受けるとともに、実験遂行時にはプロトコルを遵守する。同様に、DNA を取り扱う実験を行う場合は同様に承認を受け、環境問題および実験者の安全に十分配慮して行った。

C. 研究結果

肝臓における炎症反応は様々な薬物、外科的処置や外部刺激に起因して誘導されることが報告されているが、惹起される炎症反応の重症性、持続期間、並びにその誘導機構は多岐に渡る。そこで本節では、炎症反応のモデル薬物としてリポポリサッカライド(LPS)を腹腔内投与して作製した急性肝炎モデルに対し、マンノース修飾バブルリポソームと超音波(US) 照射の併用によってマンノース受容体発現細胞である肝血管内皮細胞に ICAM-1 siRNA を送達による抗炎症効果の評価を行った。

1-a ICAM-1 に対する siRNA 配列の最適化

siRNA を用いた疾患治療においては、標的遺伝子の発現抑制効率の増強のみならず、off-target 効果の有無を確認する上でも、siRNA 配列の最適化が重要である。そこで本研究では、100 ng/mL LPS 処置を施したマウス肝血管内皮細胞初代培養系を用いて、3 種類配列の ICAM-1 siRNA 並びに scrambled siRNA (Fig. 1A) による ICAM-1 の発現抑制効果を定量的 PCR 法により検討した。

LPS 処置の 24 時間前に静電的相互作用を介した高効率なトランスフェクション可能な汎用試薬である Lipofectamine® 2000 の推奨プロトコルに従い各 siRNA をトランスフェクションし検討した。

その結果、Fig. 1B に示すように 3 種類の ICAM-1 siRNA 全てにおいて顕著な icam-1 mRNA の発現抑制が認められ、特に sequence 1 の siRNA において最も高い icam-1 mRNA 発現抑制効果が認められた。一方、本研究において選択した scrambled siRNA において、icam-1 mRNA の発現抑制効果は認められなかったことから(Fig. 1B)、off-target 効果による ICAM-1 発現抑制ではなく、配列特異的な遺伝子ノックダウン効果であることが示唆された。

以上、本研究においては sequence 1 の siRNA 並びに上記 scrambled siRNA を用いて以下の検討を行った。

A

sequence 1	sense: GAAAGAUCAGGAUAUACAAdTdT antisense: UUGUAUAUCCUGAUCUUUCdTdT
sequence 2	sense: CAGAGAAAGAUCAGGAUAUdTdT antisense: AUAUCCUGAUCUUUCUCUGdTdT
sequence 3	sense: GUACUGUACCACUCUCAAAdTdT antisense: UUUGAGAGUGGUACAGUACdTdT
scrambled	sense: AAAUUAAAAUGCGGAACAGdTdT antisense: CUGUUCCGCAUUUUAAUUUdTdT

B

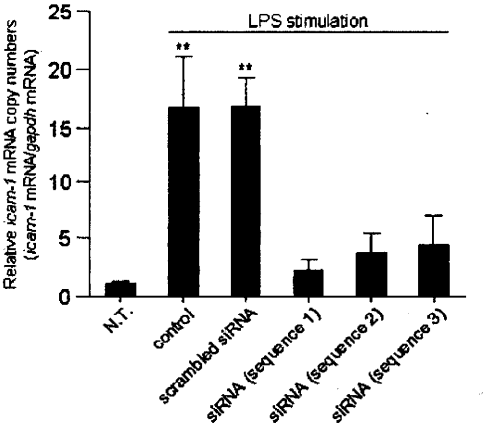

Fig. 1 ICAM-1に対するsiRNA配列デザイン (A) とLPSで刺激したマウス肝類洞血管内皮細胞初代培養系における*icam-1* mRNAの発現抑制効果 (B)

1-b 初代培養マウス肝血管内皮細胞における ICAM-1 発現抑制効果

まず in-vitro において、LPS 処置により ICAM-1 発現を誘導させた初代培養マウス肝血管内皮細胞に対し、マンノース修飾バブルリポソームと超音波照射を利用した ICAM-1 siRNA 送達による ICAM-1 発現抑制効率を検討した。ICAM-1 siRNA を用いて超音波応答性リポソーム複合体を作製した。

その結果、パーフルオロプロパンの封入に伴い溶液の白濁が認められ、リポソーム複合体内への超音波造影ガスの封入が確認された。また、ICAM-1 siRNA を用いて作製した各種リポソーム複合体の物理化学的特性を粒子径並びに表面電荷測定は、未修飾バブルリポソーム/siRNA 複合体及びマンノース修飾バブルリポソーム/siRNA 複合体の粒子径及び表面電荷はそれぞれ 106.3 ± 5.9 nm、47.2 ± 4.2 mV 及び108.0 ± 6.2 nm、49.7 ± 6.2 mV であった。また、未修飾バブルリポソーム/siRNA 複合体及びマ

ンノース修飾バブルリポソーム/siRNA 複合体の粒子径及び表面電荷はそれぞれ 545 ± 29 nm、49.8 ± 7.8 mV 及び 547 ± 16 nm、47.0 ± 3.8 mV であった。これらの複合体の物理化学的性質の値は、以前の pDNA 複合体における知見と良く一致するものである。

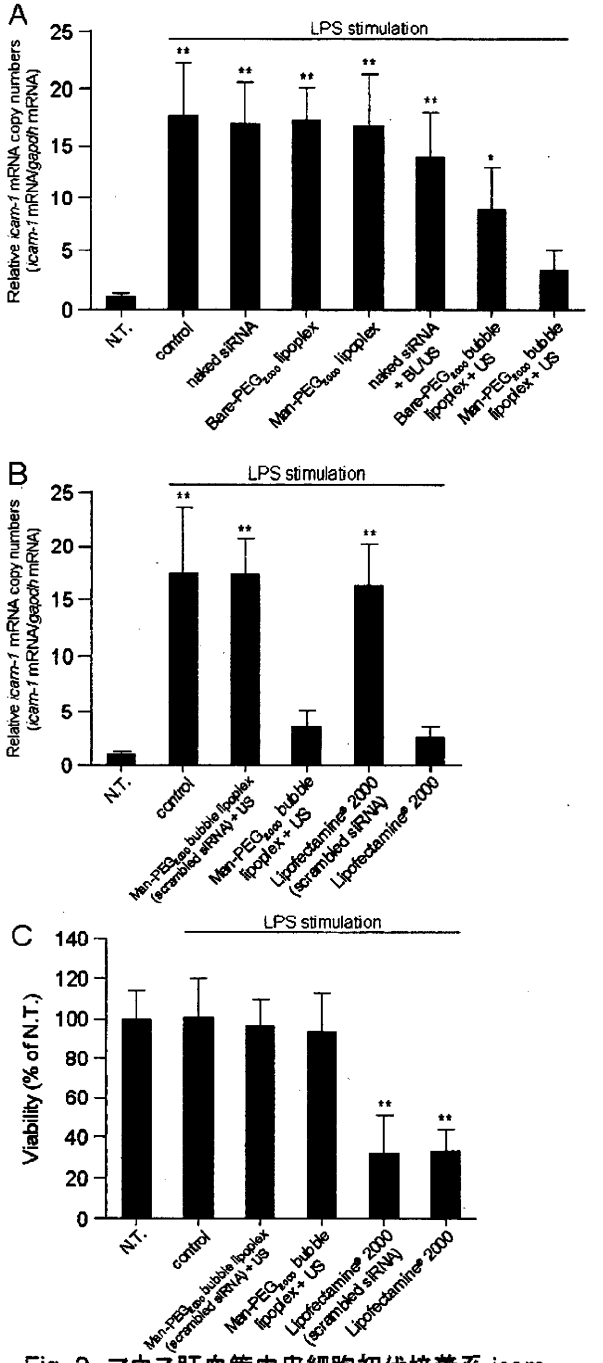

Fig. 2 マウス肝血管内皮細胞初代培養系 icam-1 mRNA発現の遺伝子ノックダウン効果に及ぼす各種製剤の影響 (A, B) と細胞毒性 (C)

次に、LPS 処置の 24 時間前に各核酸導入法を用いて ICAM-1 siRNA を初代培養マウス肝血管内皮細胞に送達した結果、マウス肝血管内皮細胞における *icam-1* mRNA 発現は、マンノース修飾バブルリポソーム/siRNA 複合体の単独添加時や naked ICAM-1 siRNA とバブルリポソーム/超音波(US)照射を併用する従来のソノポレーション法、未修飾バブルリポソームと超音波(US)照射の併用による ICAM-1 siRNA 送達時と比較して、マンノース修飾バブルリポソームと超音波照射を利用した ICAM-1 siRNA 送達により最も顕著に抑制されることが示された(Fig. 2A)。本結果は、マンノース修飾バブルリポソームと超音波(US)照射の併用による ICAM-1 siRNA 送達においても、超音波応答性リポソーム/siRNA 複合体化、並びにマンノース修飾による標的細胞との相互作用に増大に伴い、標的細胞内核酸導入効率の増強が得られることを示唆している。また、これらの結果は scrambled siRNA では認められず、本方法による *icam-1* mRNA 発現抑制効果は ICAM-1 siRNA に起因することも確認できた。さらにマンノース修飾バブルリポソーム/siRNA 複合体と超音波(US)照射による ICAM-1 siRNA 送達に伴う *icam-1* mRNA 発現抑制効果は、核酸導入試薬として汎用される Lipofectamine® 2000 に匹敵した(Fig. 2B)、一方、核酸導入に伴う細胞毒性は、高効率なトランスフェクション可能な汎用試薬である Lipofectamine® 2000 において有意に認められたが、マンノース修飾バブルリポソーム/siRNA 複合体と超音波(US)照射による送達法ではほとんど認められなかった(Fig. 2C)。

1-c ICAM-1 siRNA の肝臓内分布特性

LPS誘導急性肝炎モデルにおいて、炎症反応発生初期には肝臓の血管内皮細胞上にICAM-1が発現誘導され、好中球の血管内皮細胞との接着、回転、並びに組織内浸潤等に関与する。従って、in-vivoにおいて肝血管内皮細胞選択的なICAM-1 siRNA送達を達成することが、ICAM-1発現抑制に基づく抗炎症治療のために不可欠であるので、次にマンノース修飾バブルリポソームと超音波照射によるsiRNA送達後のICAM-1 siRNAの肝臓内分布特性を検討した。マンノース修飾バブルリポソーム/siRNA複合体と超音波(US)照射併用によりAlexa-488標識ICAM-1 siRNAを送達し、1時間後にコラゲナーゼ灌流により肝臓を実質細胞と非実質細胞に分画した。さらに肝非実質細胞をマイクロビーズ標識抗マウスF4/80抗体並びにCD146(LSEC)抗体を用いた磁気細胞分離法によりKupffer細胞と肝血管内皮細胞に分画し、それぞれの画分におけるAlexa-488由来の蛍光強度を測定した。

その結果、マンノース修飾バブルリポソームと超音波(US)照射を利用したICAM-1 siRNA送達に

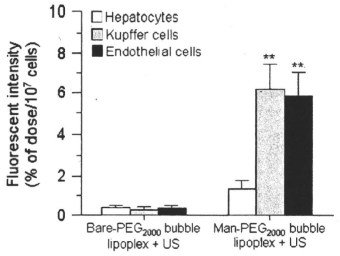

Fig. 3 マウスへ各種製剤を静脈内投与し、超音波照射後の肝臓内細胞分布

より、マンノース受容体発現細胞であるKupffer細胞と肝血管内皮細胞において得られるICAM-1 siRNA移行量は、マンノース受容体非発現細胞である肝実質細胞と比較して顕著に高いことが明らかとなった (Fig. 3)。一方、未修飾バブルリポソームと超音波(US)照射の併用によるICAM-1 siRNA送達では、マンノース受容体発現の有無によるICAM-1 siRNA移行量の差異は認められず、マンノース修飾バブルリポソームと超音波(US)照射を用いた方法では、ICAM-1発現抑制に基づく抗炎症療法の標的細胞となる肝血管内皮細胞に対する効率的なICAM-1 siRNA送達が可能であることが示された。

1-d 肝臓における ICAM-1 発現抑制効果

次に、LPS/D-ガラクトサミン腹腔内投与に伴う炎症反応の惹起により ICAM-1 発現を誘導させたマウスに対し、マンノース修飾バブルリポソームと超音波照射を利用して ICAM-1 siRNA を送達することによる ICAM-1 発現抑制効果を評価した。各核酸導入法を用いてマウスに対し ICAM-1 siRNA を送達した 24 時間後に LPS/D-ガラクトサミンを腹腔内投与し、その 3 時間後に肝血管内皮細胞を単離して細胞内 *icam-1* mRNA、並びに細胞膜上における ICAM-1 発現量を評価した。

その結果、マンノース修飾バブルリポソームと超音波(US)照射を利用した ICAM-1 siRNA 送達により肝血管内皮細胞において得られる *icam-1* mRNA 発現量は、マンノース修飾リポソーム/siRNA 複合体、naked ICAM-1 siRNA とバブルリポソームを併用する従来のソノポレーション法、未修飾バブルリポソーム/siRNA 複合体と超音波(US)照射併用による ICAM-1 siRNA 送達時と比較して顕著に低いことが示された (Fig. 4A)。また細胞膜上の ICAM-1 タンパク質発現についても ELISA 法により評価した結果、マンノース修飾バブルリポソーム

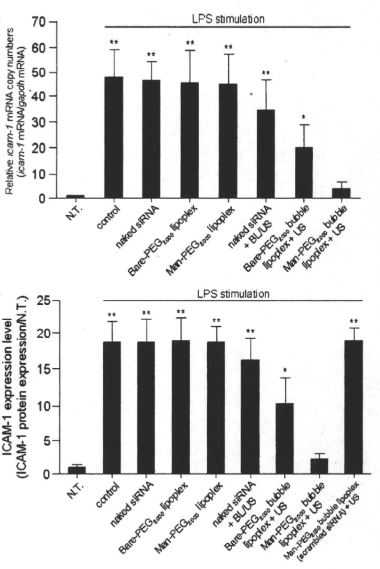

Fig. 4 LPS誘発性肝炎モデルマウスへ各種製剤を静脈内投与、超音波照射後の肝臓類洞血管内皮細胞におけるICAM-1 mRNA (A) およびICAM-1 タンパク質発現の評価(B)

と超音波(US)照射により ICAM-1 siRNA を送達することで、最も高い ICAM-1 発現抑制効果が得られた(Figs. 4B)。また、同様の結果は、ウエスタンブロティング法でも確認された (data not shown)。一方、これらの結果は scrambled siRNA では認められず、本方法による *icam-1* mRNA 及び ICAM-1 発現抑制効果は ICAM-1 siRNA に起因することも確認された。従って、マンノース修飾バブルリポソーム/siRNA 複合体と超音波(US)照射を利用した ICAM-1 siRNA 送達法によって、LPS 誘導急性肝炎モデルにおける ICAM-1 発現誘導を効率的に抑制可能であり、LPS 刺激に起因する炎症反応を抑制できる可能性が示唆された。

1-e 組織内への好中球浸潤、並びに炎症性サイトカイン産生抑制効果

LPS 誘導急性肝炎の発生初期においては、肝血管内皮細胞上に ICAM-1 が発現し、それに伴い好中球等の組織内浸潤が惹起され、その後浸潤した好中球等より好中球及び単球走化性因子の分泌、並びに炎症性サイトカイン産生が誘導される。そこでマンノース修飾バブルリポソーム/siRNA 複合

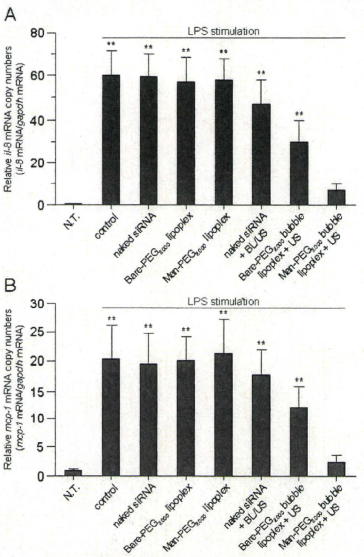

Fig. 5 LPS誘発性肝炎モデルマウスへ各種製剤を静脈内投与、超音波照射後の肝臓における *il8* mRNA (A) および *mcp-1* mRNAの評価(B)

体と超音波(US)照射を利用した ICAM-1 siRNA による ICAM-1 発現抑制に伴う、LPS/D-ガラクトサミン誘導急性肝炎モデルマウスにおける好中球の組織内浸潤抑制効果を評価した。ICAM-1 siRNA 送達 24 時間後に LPS/D-ガラクトサミンを腹腔内投与し、その 6 時間後に肝臓における好中球走化性因子 *il-8* mRNA 並びに単球走化性因子 *mcp-1* mRNA を評価した。

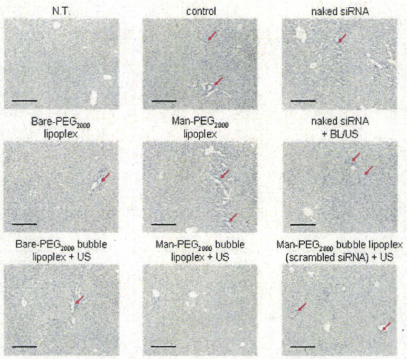

Fig. 6 LPS誘発性肝炎モデルマウスへ各種製剤を静脈内投与、超音波照射後の肝臓における好中球浸潤の評価

その結果、他の核酸送達法と比較し、マンノース修飾バブルリポソームと超音波(US)照射を利用した ICAM-1 siRNA 送達によって、肝臓中 *il-8* 及び *mcp-1* mRNA 発現量が最も効率的に抑制されることが明らかとなった(Fig. 5)。また naphthol AS-D chloroacetate 法により組織内に浸潤した好中球の染色後に顕微鏡観察した結果、マンノース修飾バブルリポソームと超音波(US)照射を利用して ICAM-1 siRNA を送達したマウス肝臓において、好中球浸潤の程度が最も低いことも示された(Fig. 6)。

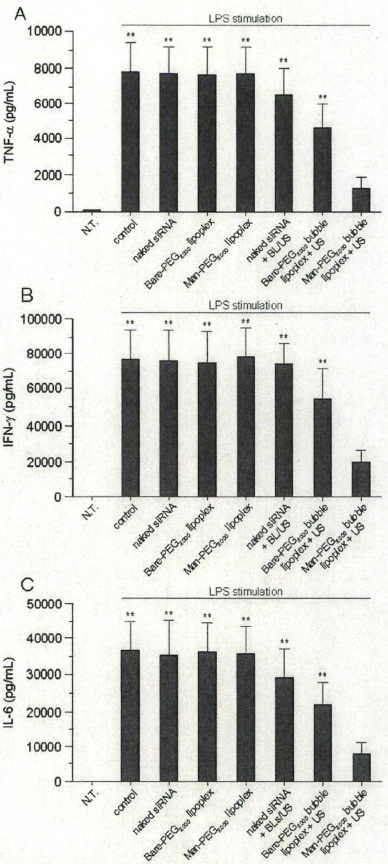

Fig. 7 LPS誘発性肝炎モデルマウスへ各種製剤を静脈内投与、超音波照射後の血清における TNFα (A), IFNγ (B), IL-6 (C) 濃度の評価

次に、マンノース修飾バブルリポソーム/と超音波(US)照射を用いた ICAM-1 siRNA による ICAM-1 発現抑制に伴う血清中炎症性サイトカイン分泌量を評価した。ICAM-1 siRNA 送達 24 時間後に LPS/D-ガラクトサミンを腹腔内投与し、その 12 時間後の血清中炎症性サイトカイン量を評価した結果、血清中 TNF-α、IFN-γ及び IL-6 濃度はマンノース修飾バブルリポソームと超音波(US)照射を利用して ICAM-1 siRNA を送達することで最も効率的に抑制されることが明らかとなった (Fig. 7)。さらにマンノース修飾バブルリポソームと超音波照射を利用した ICAM-1 siRNA 送達に伴い得られるこれらの結果は、scrambled siRNA ではいずれも認められなかった(data not shown)。従って、マンノース修飾バブルリポソームと超音波(US)照射を利用した ICAM-1 siRNA 送達による ICAM-1 発現抑制に伴い、LPS 誘導急性肝炎モデルマウスにおける炎症反応の惹起に関与する好中球の組織内浸潤、並びに炎症性サイトカイン産生が顕著に抑制されることが示された。

1-f 肝毒性評価

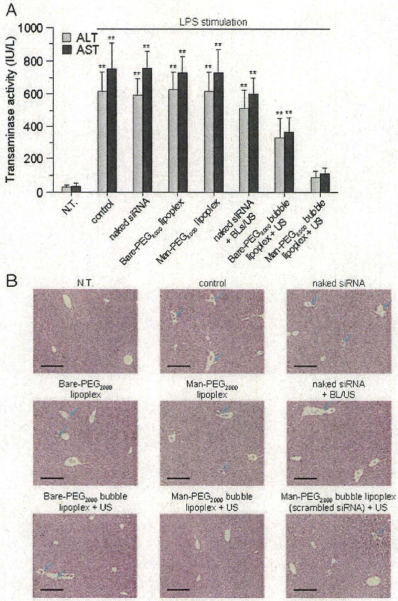

Fig. 8 LPS誘発性肝炎モデルマウスへ各種製剤を静脈内投与、超音波照射後の血清におけるALT, AST活性 (A)と肝臓組織切片観察(B)の評価

さらにマンノース修飾バブルリポソームと超音波(US)照射を利用した ICAM-1 siRNA 送達による ICAM-1 発現抑制に伴う LPS 誘導急性肝炎の抑制効果を、血清中トランスアミナーゼ活性並びに Hematoxylin-Eosin (H&E) 染色に基づく組織学的評価により検討した。まずマンノース修飾バブルリポソームと超音波(US)照射を利用した ICAM-1 siRNA 送達に伴い、LPS/D-ガラクトサミン誘導急性肝炎モデルマウスに対して得られる血清中トランスアミナーゼ活性の抑制効果を検討するために、ICAM-1 siRNA 送達24時間後にLPS/D-ガラクトサミンを腹腔内投与し、その 24 時間後の血清中 ALT, AST 活性を測定した。その結果、マンノース修飾バブルリポソームと超音波(US)照射を利用して ICAM-1 siRNA を送達したマウスにおいて、血清中 ALT, AST 活性が最も顕著に抑制されることが示された(Fig. 8A)。また肝臓の H&E 染色後に顕微鏡観察した結果、LPS 誘導急性肝炎モデルマウスの肝臓においては肝血管構造の変化、特に肝血管内皮細胞構造の崩壊が認められた一方、マンノース修飾バブルリポソームと超音波(US)照射により ICAM-1 siRNA を送達したマウス肝臓では上記のような構造変化は観察されず、未処置のマウス肝臓と同様の H&E 染色像が観察された(Fig. 8B)。以上の知見より、マンノース修飾バブルリポソームと超音波(US)照射を利用した ICAM-1 siRNA 送達では、肝血管内皮細胞における効率的な ICAM-1 発現抑制に伴う好中球の組織内浸潤、並びに炎症性サイトカイン産生の抑制に基づき、LPS 刺激に起因する炎症反応を効果的に抑制できることが示唆された。

ここまでマンノース修飾バブルリポソームと超音波(US)照射を使用したICAM-1 siRNA送達によって、炎症反応のモデル薬物として汎用されるLPSに起因した急性肝炎モデルに対して高い抗炎症効果が得られることを明らかにした。しかしながら、臨床においては様々な薬物のみならず外科的処置等によっても炎症反応が誘導されるため、マンノース修飾バブルリポソームと超音波(US)照射を利用したICAM-1 siRNA送達による抗炎症療法の臨床応用可能性を検討するためには、多種多様な炎症モデルに対して有効であることを示す必要がある。そこで、四塩化炭素(CCl_4)、ジメチルニトロソアミン(DMN)誘導急性肝炎、並びに虚血再灌流(ischemia-reperfusion; IR)性肝傷害モデルマウスにおいても、マンノース修飾バブルリポソームと超音波照射を利用したICAM-1 siRNA送達による抗炎症効果の評価を行った。

2-a　各種炎症反応に伴うICAM-1発現の抑制効果

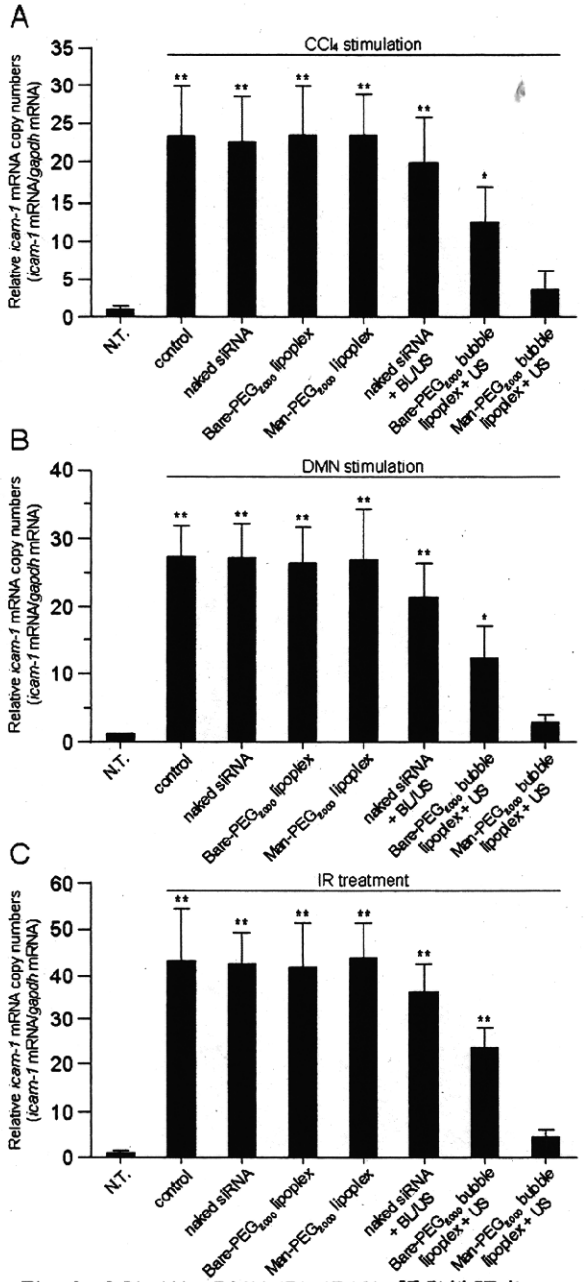

Fig. 9 CCl_4 (A), DMN (B), IR(C) 誘発性肝炎モデルマウスへ各種製剤を静脈内投与、超音波照射後の肝臓類洞血管内皮細胞におけるicam-1 mRNAの評価

まず、各種炎症反応に伴いICAM-1が発現誘導されたマウスに対し、マンノース修飾バブルリポソームと超音波(US)照射を併用してICAM-1 siRNAを送達することによるICAM-1発現抑制効果を検討した。各核酸導入法を用いてマウスに対しICAM-1 siRNAを送達した 24 時間後にCCl_4、DMN投与並びにIR処置を行い、その 6 時間後に肝血管内皮細胞を単離して細胞内*icam-1* mRNA発現量を評価した結果、いずれの急性肝炎・肝傷害モデルマウスにおいても、肝血管内皮細胞内*icam-1* mRNA発現は、マンノース修飾バブルリポソームと超音波(US)照射を利用してICAM-1 siRNAを送達により、最も効果的に抑制された(Fig. 9)。またマンノース修飾バブルリポソームと超音波(US)照射を利用したICAM-1 siRNA送達によって得られた本結果は、scrambled siRNAでは認められなかった（data not shown）。従って、マンノース修飾バブルリポソームと超音波(US)照射を利用したICAM-1 siRNA送達によるICAM-1発現抑制効果は、LPS誘導肝炎のみならず様々な急性肝炎及び肝傷害に対しても認められることが示唆された。

2-b　肝毒性評価

さらに、マンノース修飾バブルリポソームと

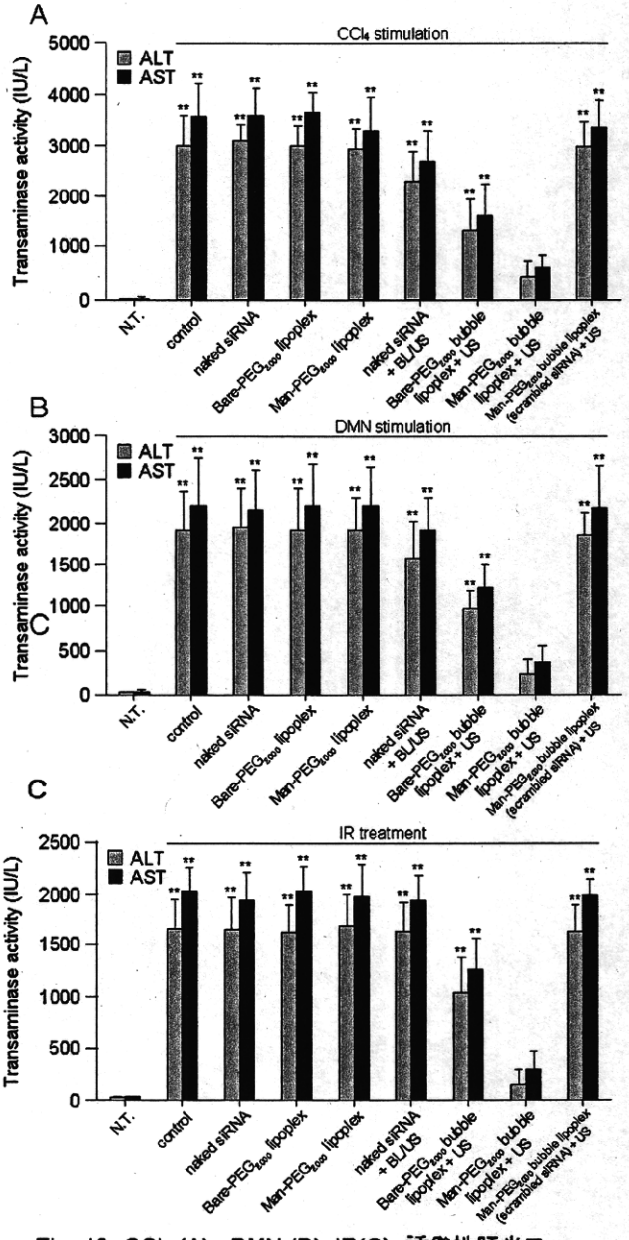

Fig. 10 CCl_4 (A), DMN (B), IR(C) 誘発性肝炎モデルマウスへ各種製剤を静脈内投与、超音波照射後の血清中ALT, AST活性の評価

超音波(US)照射を利用したICAM-1 siRNA送達によるICAM-1発現抑制に伴う各種急性肝炎･肝傷害モデルマウスにおける炎症反応抑制効果を、血清中トランスアミナーゼ活性測定により評価した。様々な核酸導入法を用いたICAM-1 siRNA送達 24 時間後にCCl_4、DMN投与並びにIR処置を行い、その 24 時間後の血清中ALT, AST活性を測定した。

その結果、いずれの急性肝炎･肝傷害モデルマウスにおいても、マンノース修飾バブルリポソームと超音波(US)照射を利用したICAM-1 siRNA送達により血清中ALT/AST活性が最も顕著に抑制された(Fig. 10)。以上の知見より、マンノース修飾バブルリポソームと超音波照射を利用したICAM-1 siRNA送達による急性炎症反応抑制効果は、LPS誘導急性肝炎のみならず様々な急性肝炎及び肝傷害に対しても認められることが示された。

D. 考察

本章では、マンノース修飾バブルリポソームと超音波(US)照射を利用した遺伝子導入法をsiRNA送達に応用し、肝血管内皮細胞内にICAM-1 siRNAを効率的に送達することによる、各種炎症反応に対する抗炎症効果を評価した。

Off-target効果、並びにTLR-3/7/8とsiRNAの相互作用に基づく炎症反応は、siRNA活性を評価する上で排除されるべき現象であり、かつsiRNA医薬の臨床応用に向けて克服すべき問題である。本研究では、3種類のICAM-1 siRNA並びにscrambled siRNAについてICAM-1の発現抑制効果を検討した結果 (Fig. 1A)、scrambled siRNAを除く全てのICAM-1 siRNAにおいて高いICAM-1発現抑制効果、並びに炎症反応の抑制効果が認められ(Fig. 1B)、off-target効果によるICAM-1発現抑制の可能性が極めて低いことを、治療効果の検討に先立ち確認した。またIFN-γ産生等の炎症反応は、エンドソーム内でのTLR-3/7/8との相互作用により惹起されるが、マンノース修飾バブルリポソームと超音波照射を使用したsiRNA送達では、製剤への超音波照射に伴う細胞穿孔によって細胞質内にsiRNAが直接導入されるため、本方法においてはTLR分子種との相互作用に伴う炎症反応の惹起を考慮する必要がないと考えられる。一方、siRNAは細胞質内に存在するRIG-1等にも認識され炎症反応を誘発すると考えられるので、本研究においては、RIG-1経路の下流に存在する転写因子IRF3/7の活性化を抑制できることが報告されている3'末端へのオーバーハング配列(dTdT)をsiRNAに付与することでその影響を抑えることとした。このように、本方法では超音波照射に伴う超音波(US)応答性リポプレックスの崩壊に伴う細胞膜上に一過性に生じる小孔を介してsiRNAが細胞質内に直接導入され、従来のリポフェクション法によるsiRNA送達において障壁とされていたエンドソーム脱出効率の低さやエンドソーム内での分解等を考慮する必要がなく、siRNAが直接送達される細胞質内はsiRNAの機能発現部位であるため、本方法は高効率かつ細胞選択的なsiRNA送達法として優れた特性を有する。

マンノース修飾バブルリポソームと超音波照射を利用したICAM-1 siRNA送達では、ICAM-1発現を惹起するLPS処置を施した初代培養マウス肝血管内皮細胞において、マンノース修飾バブルリポソームと超音波照射を利用したICAM-1 siRNA送達により、他の方法を用いてICAM-1 siRNAを送達した場合と比較して、細胞内*icam-1* mRNA発現が最も抑制されることが明らかとなった (Fig. 4)。またin-vivoにおいても、ICAM-1発現が惹起されるLPS誘導急性肝炎モデルマウスにおいて、マンノース修飾バブルリポソームと超音波照射を利用したICAM-1 siRNA送達後のマウス肝血管内皮細胞におけるICAM-1発現抑制効率を評価した結果、細胞内*icam-1* mRNA発現量、並びに細胞膜上のICAM-1発現量共に最も顕著に抑制されることが明らかとなった(Fig. 4)。さらに本方法を用いたICAM-1 siRNA送達によるICAM-1発現抑制に伴い、好中球の組織内浸潤、並びに炎症性サイトカイン産生を抑制でき(Figs. 5-7)、その結果LPS誘導急性肝炎モデルマウスの炎症反応を顕著に抑制できることが明らかとなった(Fig. 8)。マンノース修飾バブルリポソーム/siRNA複合体と超音波照射を用いた方法では、以前のpDNA複合体送達における我々の知見と同様、標的細胞となる肝臓及び脾臓のマンノース受容体発現細胞への選択的かつ高効率なsiRNA送達により、ICAM-1発現抑制に基づく抗炎症療法の標的細胞となる肝血管内皮細胞に対する効率的なICAM-1 siRNA送達が可能であると考えている。実際、本研究で用いたsiRNA量は10 μg/mouse (0.5 mg/kg)であり、少量の投与により治療効果を得ることができた。これは、本DDS製剤による高効率かつ細胞選択的なsiRNA送達性を強く支持するものである。

一方、LPSは急性炎症反応を惹起するためのモデル薬物として汎用されるが、臨床においては様々な薬物のみならず外科的処置や物理刺激等によっても炎症反応が誘導される。従って、マンノース修飾バブルリポソームと超音波(US)照射を利用したICAM-1 siRNA送達による抗炎症療法の臨床応用の可否を検討するためには、多種多様な炎症モデルに対する効果を評価する必要がある。そこで、CCl_4、DMN誘導急性炎症、並びにIR性肝傷害に対する抗炎症効果を評価した。その結果、

いずれの急性肝炎･肝傷害モデルマウスにおいても、マンノース修飾バブルリポソームと超音波(US)照射を利用してICAM-1 siRNAを送達することで、高い肝血管内皮細胞内*icam-1* mRNA発現抑制効果を示し(Fig. 9)、それに伴い各種急性肝炎モデルマウスの炎症反応を顕著に抑制できることが明らかとなった(Fig. 10)。LPS、CCl_4及びDMN投与並びにIR処置に伴う炎症反応の詳細な発生機序は異なるが、炎症反応発生過程における肝血管内皮細胞上へのICAM-1発現誘導は本研究において使用した薬物やIR処置のみならず、様々な刺激誘導性炎症反応においても報告されている。従って、マンノース修飾バブルリポソームと超音波(US)照射を利用したICAM-1 siRNA送達による抗炎症治療では、様々な急性肝炎及び肝傷害に対して高い効果が期待できると考えられる。

siRNAを用いた疾患治療においては、遺伝子発現抑制効果のみならず、その抑制効果持続時間も重要な因子である。一般的に細胞質内に導入されたsiRNAは細胞分裂に伴う希釈やヌクレアーゼ等生体固有のRNA分解機構により速やかに消失する。本研究では、急性炎症を標的疾患としているため遺伝子発現抑制時間を考慮する必要はないが、来年度以降、本DDSを利用したsiRNAの肝星（伊東）細胞への細胞送達法による肝硬変治療への応用には、生体内におけるsiRNA分解を抑制するためにコレステロール修飾や、2'-4'間に架橋構造を有するLocked Nucleic Acid(LNA)の導入等を検討する必要があるかもしれない。

マンノース修飾バブルリポソームと超音波(US)照射によりICAM-1 siRNAを肝血管内皮細胞に対し選択的かつ高効率に送達することで、様々な刺激誘導性炎症反応に対する抗炎症効果を得られることが明らかとなった。急性肝炎は様々な薬物治療と共に偶発的に発生し、またIR処置に伴う炎症反応は生体肝移植時における問題点として知られている。マンノース修飾バブルリポソームと超音波(US)照射によるICAM-1 siRNA送達に基づく抗炎症療法は、siRNAに起因した有害作用が低く、かつ様々な炎症反応に対して広く適応できる可能性を秘めているので、炎症反応が懸念される疾患治療前に本DDSによりICAM-1 siRNAを送達することで、炎症反応の発生を抑止できると考えられる。

E．結論

超音波(US)応答性マンノース修飾バブルリポソームを用いたsiRNAの肝臓類洞血管内皮細胞への高効率な細胞選択的送達法の構築に成功した。また、ICAM-1 siRNAを送達することで、LPS誘発性肝炎、CCl_4、DMN誘導急性炎症、並びにIR性肝傷害モデルマウスにおいて有意な抗炎症効果を発揮することが示された。

F．健康危険情報　なし

G．研究発表

1.　論文発表

1．K. Un, S. Kawakami, R. Suzuki, K. Maruyama, F. Yamashita, and M. Hashida: Development of an ultrasound-responsive and mannose-modified gene carrier for DNA vaccine therapy,
Biomaterials, 31 (30), 7813-7826 (2010)

2. K. Un, S. Kawakami†, R. Suzuki, K. Maruyama, F. Yamashita, and M. Hashida†: Suppression of melanoma growth and metastasis by DNA vaccination using an ultrasound-responsive and mannose-modified gene carrier, († corresponding authors)
Molecular Pharmaceutics, 8 (2), 543-554 (2011)

2.　学会発表

1. 運 敬太、川上 茂、樋口ゆり子、鈴木亮、丸山一雄、山下富義、橋田 充：超音波応答性マンノース修飾リポソームを用いたsiRNA送達システムにおける新規抗炎症療法の開発、第26回日本DDS学会(1-D-21)、大阪、6月17-18日

2. S. Kawakami, K. Un, R. Suzuki, K. Maruyama, Y. Higuchi, F. Yamashita, and M. Hashida: Gene transfection characteristics of an ultrasound-responsive and mannose-modified bubble lipoplex, International Conference on Biomaterials Science (ICBS) 2011, March 15-18, 2011, Tsukuba, Japan.

H．知的財産権の出願・登録状況

（予定を含む。）

1. 特許取得　　なし
2. 実用新案登録　　なし
3. その他　　なし

研究成果の刊行に関する一覧表

書籍

著者氏名	論文タイトル名	書籍全体の編集者名	書　籍　名	出版社名	出版地	出版年	ページ

雑誌

発表者氏名	論文タイトル名	発表誌名	巻号	ページ	出版年
K. Un, S. Kawakami, R. Suzuki, K. Maruyama, F. Yamashita, M. Hashida	Development of an ultrasound-responsive and mannose-modified gene carrier for DNA vaccine therapy	*Biomaterials*	31 (30)	7813-7826	2010
K. Un, S. Kawakami†, R. Suzuki, K. Maruyama, F. Yamashita, M. Hashida† († corresponding authors)	Suppression of melanoma growth and metastasis by DNA vaccination using an ultrasound-responsive and mannose-modified gene carrier	*Molecular Pharmaceutics*	8 (2)	543-554	2011

Biomaterials 31 (2010) 7813–7826

Contents lists available at ScienceDirect

Biomaterials

journal homepage: www.elsevier.com/locate/biomaterials

Development of an ultrasound-responsive and mannose-modified gene carrier for DNA vaccine therapy

Keita Un [a,b], Shigeru Kawakami [a], Ryo Suzuki [c], Kazuo Maruyama [c], Fumiyoshi Yamashita [a], Mitsuru Hashida [a,d,*]

[a] Department of Drug Delivery Research, Graduate School of Pharmaceutical Sciences, Kyoto University, 46-29 Yoshida-shimoadachi-cho, Sakyo-ku, Kyoto 606-8501, Japan
[b] The Japan Society for the Promotion of Science (JSPS), Chiyoda-ku, Tokyo 102-8471, Japan
[c] Department of Biopharmaceutics, School of Pharmaceutical Sciences, Teikyo University, 1091-1 Suwarashi, Sagamiko, Sagamihara, Kanagawa 229-0195, Japan
[d] Institute for Integrated Cell-Material Sciences (iCeMS), Kyoto University, Yoshida-ushinomiya-cho, Sakyo-ku, Kyoto 606-8302, Japan

ARTICLE INFO

Article history:
Received 31 May 2010
Accepted 29 June 2010
Available online 24 July 2010

Keywords:
Gene transfer
Bubble lipoplexes
Ultrasound exposure
Mannose receptors
Antigen presenting cells
DNA vaccine therapy

ABSTRACT

Development of a gene delivery system to transfer the gene of interest selectively and efficiently into targeted cells is essential for achievement of sufficient therapeutic effects by gene therapy. Here, we succeeded in developing the gene transfection method using ultrasound (US)-responsive and mannose-modified gene carriers, named Man-PEG_{2000} bubble lipoplexes. Compared with the conventional lipofection method using mannose-modified carriers, this transfection method using Man-PEG_{2000} bubble lipoplexes and US exposure enabled approximately 500~800-fold higher gene expressions in the antigen presenting cells (APCs) selectively in vivo. This enhanced gene expression was contributed by the improvement of delivering efficiency of nucleic acids to the targeted organs, and by the increase of introducing efficiency of nucleic acids into the cytoplasm followed by US exposure. Moreover, high antitumor effects were demonstrated by applying this method to DNA vaccine therapy using ovalbumin (OVA)-expressing plasmid DNA (pDNA). This US-responsive and cell-specific gene delivery system can be widely applied to medical treatments such as vaccine therapy and anti-inflammation therapy, which its targeted cells are APCs, and our findings may help in establishing innovative methods for in-vivo gene delivery to overcome the poor introducing efficiency of carriers into cytoplasm which the major obstacle associated with gene delivery by non-viral carriers.

© 2010 Elsevier Ltd. All rights reserved.

1. Introduction

In the post-genome era, the analysis of disease-related genes has rapidly advanced, and the medical application of the information obtained from gene analysis is being put into practice. In particular, the development of effective method to transfer the gene of interest selectively and efficiently into the targeted cells is essential for the gene therapy of refractory diseases, in-vivo functional analysis of genes and establishment of animal models for diseases. However, a suitable carrier for selective and efficient gene transfer to the targeted cells is still being developed. Although various types of viral and non-viral carriers have been developed for gene transfer, they are limited to use by viral-associated pathogenesis and low transfection efficiency, respectively. For the cell-selective gene transfer, many investigators have focused on ligand-modified non-viral carriers such as liposomes [1–4], emulsions [5], micelles [6] and polymers [7], because of their high productivity and low toxicity. On the other hand, since the gene transfection efficiency by non-viral carriers is poor, it is difficult to obtain the effective therapeutic effects by gene therapy using non-viral carriers. Moreover, in the gene transfection using conventional ligand-modified non-viral carriers, since the carriers need to be taken up into cells via endocytosis following by interaction with targeted molecules on the cell membrane, the number of candidates which are suitable as ligands for targeted gene delivery is limited.

Some researchers have attempted to develop the transfection method using external stimulation, such as electrical energy [8], physical pressure [9] and water pressure [10], to enhance the gene transfection efficiency. Among these, gene transfection method using US exposure and microbubbles enclosing US imaging gas, called "sonoporation method", have been focused as effective drug/gene delivery systems [11–14]. In the sonoporation method, microbubbles are degraded by US exposure with optimized intensity, then cavitation energy is generated by the destruction of

* Corresponding author. Department of Drug Delivery Research, Graduate School of Pharmaceutical Sciences, Kyoto University, 46-29 Yoshida-shimoadachi-cho, Sakyo-ku, Kyoto 606-8501, Japan. Tel.: +81 75 753 4545; fax: +81 75 753 4575.
E-mail address: hashidam@pharm.kyoto-u.ac.jp (M. Hashida).

0142-9612/$ – see front matter © 2010 Elsevier Ltd. All rights reserved.
doi:10.1016/j.biomaterials.2010.06.058

microbubbles. Consequently, the transient pores are created on the cell membrane, and large amount of nucleic acids are directly introduced into the cytoplasm through the created pores [13,15,16]. However, the in-vivo gene transfection efficiency by conventional sonoporation method administering the nucleic acids and microbubbles separately is low because of the rapid degradation of nucleic acids in the body [17], the large particle size of conventional microbubbles [15] and the different pharmacokinetic profiles of the nucleic acids and microbubbles. Moreover, to transfer the gene into the targeted cells selectively by sonoporation method in vivo, the control of in-vivo distribution of nucleic acids and microbubbles, which are separately administered, is necessary.

In our previous report [16], we have demonstrated the effective transfection by combination-use method using our mannosylated lipoplexes composed of Man-C4-chol: DOPE [1], and conventional Bubble liposomes (BLs) [12] with US exposure. However, this combination-use method is complicated because of the necessity for multiple injections of mannosylated lipoplexes and BLs; therefore, it is difficult to apply for medical treatments using multiple transfections. In addition, the difference of in-vivo distribution characteristics between mannosylated lipoplexes and BLs might be decreased its transfection efficacy. Therefore, it is essential to develop the US-responsive and cell-selective gene carriers constructed with ligand-modified gene carriers and microbubbles.

Taking these into considerations, we examined the gene transfection system for effective DNA vaccine therapy using physical stimulation and ligand-modification. First, we developed US-responsive and mannose-modified gene carriers, Man-PEG_{2000} bubble lipoplexes (Fig. 1), by enclosing perfluoropropane gas into mannose-conjugated PEG_{2000}-DSPE-modified cationic liposomes (DSTAP: DSPC: Man-PEG_{2000}-DSPE (Fig. 1))/pDNA complexes. Then, we evaluated the enhanced and cell-selective gene expression in the APCs by intravenous administration of Man-PEG_{2000} bubble lipoplexes and external US exposure in mice. Finally, we examined high anti-tumor effects by applying this method to DNA vaccine therapy using OVA-expressing pDNA.

2. Materials and methods

2.1. Mice and cell lines

Female ICR mice (4~5 weeks old) and C57BL/6 mice (6~8 weeks old) were purchased from the Shizuoka Agricultural Cooperative Association for Laboratory Animals (Shizuoka, Japan). All animal experiments were carried out in accordance with the Principles of Laboratory Animal Care as adopted and promulgated by the US National Institutes of Health and the guideline for animal experiments of Kyoto University. CD8-OVA1.3 cells, T cell hybridomas with specificity for OVA 257~264-kb, were kindly provided by Dr. C.V. Harding (Case Western Reserve University, Cleveland, OH, USA) [18]. EL4 cells (C57BL/6 T-lymphomas) and E.G7-OVA cells (the OVA-transfected clones of EL4) were purchased from American Type Culture Collection (Manassas, VA). CD8-OVA1.3 cells and EL4 cells were maintained in Dulbecco's modified Eagle's medium and E.G7-OVA cells were maintained in RPMI-1640. Both mediums were supplemented with 10% fetal bovine serum (FBS), 0.05 mM 2-mercaptoethanol, 100 IU/mL penicillin, 100 μg/mL streptomycin and 2 mM L-glutamine at 37 °C in 5% CO_2.

2.2. pDNA

pCMV-Luc and pCMV-OVA were constructed in our previous reports [19,20]. Briefly, pCMV-Luc was constructed by subcloning the HindIII/Xba I firefly luciferase cDNA fragment from pGL3-control vector (Promega, Madison, WI, USA) into the polylinker of pcDNA3 vector (Invitrogen, Carlsbad, CA, USA). pCMV-OVA was constructed by subcloning the EcoRI chicken egg albumin (ovalbumin) cDNA fragment from pAc-neo-OVA, which was kindly provided by Dr. M.J. Bevan (University of Washington, Seattle, WA, USA) into the polylinker of pVAX I. pDNA were amplified in the E. coli strain DH5α, isolated and purified using a QIAGEN Endofree Plasmid Giga Kit (QIAGEN GmbH, Hilden, Germany).

2.3. Synthesis of Man-PEG_{2000}-DSPE and preparation of Man-PEG_{2000} bubble lipoplexes

Man-PEG_{2000}-DSPE was synthesized in a one-step reaction by covalent binding with NH_2-PEG_{2000}-DSPE (NOF Co., Tokyo, Japan) and 2-imino-2-methoxyethyl-1-thiomannoside (IME-thiomannoside). IME-thiomannoside was prepared according to the method of Lee [21]. Next, NH_2-PEG_{2000}-DSPE and IME-thiomannoside were reacted, vacuum dried and dialyzed to produce Man-PEG_{2000}-DSPE, and then, the resultant dialysates were lyophilized. To produce the liposomes for bubble lipoplexes, DSTAP (Avanti Polar Lipids Inc., Alabaster, AL, USA), DSPC (Sigma Chemicals Inc., St. Louis, MO, USA) and Man-PEG_{2000}-DSPE or NH_2-PEG_{2000}-DSPE were mixed in chloroform at a molar ratio of 7:2:1. For construction of BLs, DSPC and methoxy-PEG_{2000}-DSPE (NOF Co., Tokyo, Japan) were mixed in chloroform at a molar ratio of 94:6. The mixture for the construction of liposomes was dried by evaporation, vacuum desiccated and the resultant lipid film was resuspended in sterile 5% dextrose. After hydration for 30 min at 65 °C, the dispersion was sonicated for 10 min in a bath sonicator and for 3 min in a tip sonicator to produce liposomes. Then, liposomes were sterilized by passage through a 0.45 μm filter (Nihon-Millipore, Tokyo, Japan). The lipoplexes were prepared by gently mixing with equal volumes of pDNA and liposome solution at a charge ratio of 1.0:2.3 (−:+). For preparation of BLs and bubble lipoplexes, the enclosure of US imaging gas into liposomes and lipoplexes was performed according to our previous report [16]. Briefly, prepared liposomes and lipoplexes were added to 5 mL sterilized vials, filled with perfluoropropane gas (Takachiho Chemical Industries Co., Ltd., Tokyo, Japan), capped and then pressured with 7.5 mL of perfluoropropane gas. To enclose US imaging gas into the liposomes and lipoplexes, the vial was sonicated using a bath-type sonicator (AS ONE Co., Osaka, Japan) for 5 min. The particle sizes and zeta

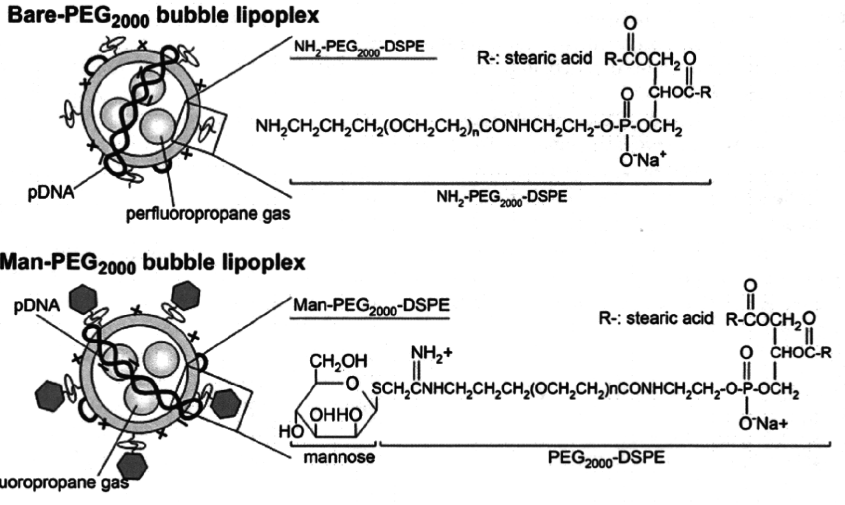

Fig. 1. Structure of Bare-PEG_{2000} bubble lipoplex containing NH_2-PEG_{2000}-DSPE and Man-PEG_{2000} bubble lipoplex containing Man-PEG_{2000}-DSPE used in this study.

potentials of liposomes and lipoplexes were determined by a Zetasizer Nano ZS instrument (Malvern Instrument, Ltd., Worcestershire, UK).

2.4. Harvesting of mouse peritoneal macrophages

Mouse peritoneal macrophages were harvested and cultured according to our previous report [16]. Briefly, the macrophages were harvested from mice at 4 days after intraperitoneal injection of 2.9% thioglycolate medium (1 mL). The collected macrophages were washed and suspended in RPMI-1640 medium supplemented with 10% FBS, 100 IU/mL penicillin, 100 μg/mL streptomycin and 2 mM L-glutamine, and plated on culture plates. After incubation for 2 h at 37 °C in 5% CO_2, non-adherent cells were washed off with culture medium, and the macrophages were incubated for another 72 h.

2.5. In-vitro gene transfection

After the macrophages were collected and incubated for 72 h, the culture medium was replaced with Opti-MEM I containing bubble lipoplexes (5 μg pDNA). The macrophages were exposed to US (frequency, 2.062 MHz; duty, 50%; burst rate, 10 Hz; intensity 4.0 W/cm^2) for 20 s using a 6 mm diameter probe placed in the well at 5 min after addition of bubble lipoplexes. In the transfection using naked pDNA and BLs, at 5 min after addition of naked pDNA (5 μg) and BLs (60 μg total lipids) were added, and the macrophages were immediately exposed to US. US was generated using a Sonopore-4000 sonicator (NEPA GENE, Chiba, Japan). Then, 1 h later, the incubation medium was replaced with RPMI-1640 and incubated for an additional 23 h. Lipofectamine® 2000 (Invitrogen, Carlsbad, CA, USA) was used according to the recommended procedures, and the exposure time of Lipofectamine® 2000 was 1 h, which is the same exposure time in other experiments using lipoplexes. Following incubation for 24 h, the cells were scraped from the plates and suspended in lysis buffer (0.05% Triton X-100, 2 mM EDTA, 0.1 M Tris, pH 7.8). Then, the cell suspension was shaken, and centrifuged at 10,000g, 4 °C for 10 min. The supernatant was mixed with luciferase assay buffer (Picagene, Toyo Ink Co., Ltd., Tokyo, Japan) and the luciferase activity was measured in a luminometer (Lumat LB 9507, EG&G Berthold, Bad Wildbad, Germany). The luciferase activity was normalized with respect to the protein content of cells. The protein concentration was determined with a Protein Quantification Kit (Dojindo Molecular Technologies, Inc., Tokyo, Japan). The level of luciferase mRNA expression was determined by RT-PCR.

2.6. Inhibitory experiments of endocytosis in vitro

Endocytosis was inhibited by chlorpromazine (50 μM) as clathrin-mediated endocytosis inhibitor [22], genistein (200 μM) as caveolae-mediated endocytosis inhibitor [23] and 5-(*N*-ethyl-*N*-isopropyl)amiloride (EIPA, 50 μM) as macropinocytosis inhibitor [24]. Each endocytosis inhibitor was added to the macrophages at 30 min before the addition of lipoplexes.

2.7. Fluorescence photographs of pDNA in mouse peritoneal macrophages

To visualize the cellular association of pDNA by fluorescence microscopy (Biozero BZ-8000, KEYENCE, Osaka, Japan), lipoplexes were constructed with TM-rhodamine-labeled pDNA prepared by a Label IT Nucleic Acid Labeling Kit (Mirus Co., Madison, WI, USA).

2.8. Evaluation of cytotoxic effects by MTT assay

The cytotoxicity was evaluated by MTT assay. Briefly, 3-(4,5-dimethyl-2-thiazol)-2,5-diphenyltetrazolium bromide (MTT, Nacalai Tesque, Inc., Kyoto, Japan) solution was added to each well and incubated for 4 h. The resultant formazan crystals were dissolved in 0.04 M HCl-isopropanol and sonicated for 10 min in a bath sonicator. Absorbance values at 550 nm (test wavelength) and 655 nm (reference wavelength) were measured and the results were expressed as viability (%).

2.9. In-vivo gene transfection

Four-week-old ICR female mice were intravenously injected with 400 μL bubble lipoplexes via the tail vein using a 26-gauge syringe needle at a dose of 50 μg pDNA. At 5 min after the injection of bubble lipoplexes, US (frequency, 1.045 MHz; duty, 50%; burst rate, 10 Hz; intensity 1.0 W/cm^2; time, 2 min) was exposed transdermally to the abdominal area using a Sonopore-4000 sonicator with a probe of diameter 20 mm. In the transfection using naked pDNA and BLs, at 4 min after intravenous injection of BLs (500 μg total lipid), naked pDNA (50 μg) was intravenously injected and US was exposed at 1 min after naked pDNA injection. At predetermined times after injection, mice were sacrificed and their organs collected for each experiment. The organs were washed twice with cold saline and homogenized with lysis buffer (0.05% Triton X-100, 2 mM EDTA, 0.1 M Tris, pH 7.8). The lysis buffer was added in a weight ratio of 5 mL/g for the liver or 4 mL/g for the other organs. After three cycles of freezing and thawing, the homogenates were centrifuged at 10,000g, 4 °C for 10 min. The luciferase activity of resultant supernatant was determined by luciferase assay and the level of luciferase mRNA expression was determined by RT-PCR.

2.10. In-vivo imaging

At 6 h after transfection, anesthetized mice were administrated D-luciferin (10 mg/300 μL PBS) (Promega Co., Madison, WI, USA). At 10 min after injection of D-luciferin, organs were excised and luminescent images were taken by NightOWL LB 981 NC instrument (Berthold Technologies, GmbH, Bad Wildbad, Germany). The pseudocolor luminescent images were generated, overlaid with organ images and the luminescence representation was obtained using WinLight software (Berthold Technologies GmbH, Bad Wildbad, Germany).

2.11. Separation of mouse hepatic PCs and NPCs

The separation of mouse hepatic PCs and NPCs was performed according to our previous reports [19]. Briefly, at 6 h after in-vivo transfection using bubble lipoplexes and US exposure, each mouse was anesthetized with pentobarbital sodium (40~60 mg/kg) and the liver was perfused with perfusion buffer (Ca^{2+}, Mg^{2+}-free HEPES solution, pH 7.2) for 10 min. Then, the liver was perfused with collagenase buffer (HEPES solution, pH 7.5 containing 5 mM $CaCl_2$ and 0.05% (w/v) collagenase (type I)) for 5 min. Immediately after the start of perfusion, the vena cava and aorta were cut and the perfusion rate was maintained at 5 mL/min. At the end of perfusion, the liver was excised. The cells were dispersed in ice-cold Hank's-HEPES buffer by gentle stirring and then filtered through cotton mesh sieves, followed by centrifugation at 50g for 1 min. The pellets containing the hepatic PCs were washed five times with Hank's-HEPES buffer by centrifuging at 50g for 1 min. The supernatant containing the hepatic NPCs was similarly centrifuged 5 times and the resulting supernatant was centrifuged twice at 300g for 10 min. Then, the PCs and NPCs were resuspended separately in ice-cold Hank's-HEPES buffer.

2.12. Isolation of mouse splenic CD11c$^+$ cells

The isolation of mouse splenic CD11c$^+$ cells was performed according to our previous reports [25]. Briefly, At 6 h after in-vivo transfection using bubble lipoplexes and US exposure, the splenic cells were suspended in ice-cold RPMI-1640 medium on ice. Red blood cells were removed by incubation with hemolytic reagent (0.15 M NH_4Cl, 10 mM $KHCO_3$, 0.1 mM EDTA) for 3 min at room temperature. The CD11c$^+$ cells were isolated by magnetic cell sorting with anti-mouse CD11c (N418) microbeads and auto MACS (Miltenyi Biotec, Inc., Auburn, CA, USA) following the manufacturer's instructions.

2.13. Quantitative RT-PCR

Total RNA was isolated from separated cells using a GenElute Mammalian Total RNA Miniprep Kit (Sigma-Aldrich, St. Louis, MO, USA). Reverse transcription of mRNA was carried out using a PrimeScript® RT reagent Kit (Takara Bio Inc., Shiga, Japan). Real-time PCR was performed using SYBR® Premix Ex Taq (Takara Bio Inc., Shiga, Japan) and Lightcycler Quick System 350S (Roche Diagnostics, Indianapolis, IN, USA) with primers. The primers for luciferase and gapdh cDNA were constructed as follows: primer for luciferase cDNA, 5′-TTCTTCGCCAAAAGCACTC-3′ (forward) and 5′-CCCTCGGGTGTAATCAGAAT-3′ (reverse); primer for gapdh, 5′-TCTCCTGCGACTTCAACA-3′ (forward) and 5′-GCTGTAGCCGTATTCATTGT-3′ (reverse) (Sigma-Aldrich, St. Louis, MO, USA). The mRNA copy numbers were calculated for each sample from the standard curve using the instrument software ('Arithmetic Fit Point analysis' for the Lightcycler). The results were expressed as the ratio of luciferase mRNA copy numbers to the housekeeping gene (gapdh) mRNA copy numbers.

2.14. Tissue distribution of radio-labeled pDNA

Lipoplexes constructed with ^{32}P-labeled pDNA ([α-^{32}P]-dCTP, PerkinElmer, Inc., MA, USA) [26] were injected intravenously into mice. At predetermined times after injection, blood was collected from the vena cava under pentobarbital anesthesia. Then, mice were sacrificed and the organs were collected, rinsed with saline and weighed. The tissues were dissolved in Soluene-350 and the resultant lysates were decolorized with isopropanol and 30% H_2O_2, and then neutralized with 5 N HCl. The radioactivity of ^{32}P-labeled pDNA was measured in scintillation counter (LSA-500, Beckman Coulter, Inc., CA, USA) after addition of Clear-Sol I solution.

2.15. Measurement of transaminase activity in the serum

At predetermined times after transfection, the serum was collected from the anesthetized mice. Alanine aminotransferase (ALT) and aspartate aminotransferase (AST) activities in the serum were determined using Transaminase CII-Test Wako kit (Wako Pure Chemical Industries Ltd., Tokyo, Japan) according to manufacturer's instructions.

2.16. Antigen presenting assay

The evaluation of antigen presentation on MHC class I molecules in the splenic dendritic cells was performed by in-vitro antigen presentation assay using CD8-OVA1.3 cells, which are T cell hybridomas with specificity for OVA. The $CD11c^+$ cells isolated from immunized mice were plated in a 96-well plate at various cells numbers and co-cultured with CD8-OVA1.3 cells (1×10^5) for 20 h. The antigen presentation on MHC class I molecules was evaluated by IL-2 secreted from activated CD8-OVA1.3 cells measured by a commercial IL-2 ELISA Kit (Bay bioscience Co., Ltd., Hyogo, Japan).

2.17. Evaluation of OVA-specific cytokine secretion from the splenic cells

At 2 weeks after the last immunization, the splenic cells collected from immunized mice were plated in 96-well plates and incubated for predetermined times at 37 °C in the presence or absence of OVA (100 μg). IFN-γ and IL-4 in the culture medium were measured by the commercial ELISA Kit, respectively (Bay bioscience Co., Ltd., Hyogo, Japan).

2.18. OVA-specific CTL assay

At 2 weeks after the last immunization, the splenic cells harvested from immunized mice were plated in 6-well plates and co-incubated with mitomycin C-treated E.G7-OVA cells or EL4 cells for 4 days. After co-incubation, non-adherent cells were collected, washed and plated in 96-well plates with target cells (E.G7-OVA cells or EL4 cells) at various effector/target (E/T) ratios. The target cells were labeled with ^{51}Cr by incubating with $Na_2^{51}CrO_4$ (PerkinElmer, Inc., MA, USA) in culture medium for 1 h at 37 °C. At 4 h after incubation, the plates were centrifuged and the resultant supernatant of each well was collected and the radioactivity of released ^{51}Cr was measured in a gamma counter. The percentage of ^{51}Cr release was calculated as follows: specific (lysis (%) = [(experimental ^{51}Cr release − spontaneous ^{51}Cr release)/(maximum ^{51}Cr release − spontaneous ^{51}Cr release)] × 100). The percentage of OVA-specific ^{51}Cr release was calculated as (% of ^{51}Cr release from E.G7-OVA cells) − (% of ^{51}Cr release from EL4 cells).

2.19. Therapeutic effects

C57BL/6 mice were immunized three times biweekly. At 2 weeks after last immunization, E.G7-OVA cells and EL4 cells were transplanted subcutaneously into the back of mice. The tumor growth and survival of mice were monitored up to 80 days after transplantation of E.G7-OVA cells and EL4 cells.

2.20. Statistics

Results were presented as the mean ± SD of more than three experiments. Analysis of variance (ANOVA) was used to test the statistical significance of differences among groups. Two-group comparisons were performed by the Student's *t*-test. Multiple comparisons between control groups and other groups were performed by the Dunnett's test and multiple comparisons between all groups were performed by the Tukey-Kramer test.

3. Results

3.1. In-vitro gene transfection properties by Man-PEG_{2000} lipoplexes

Polyethylene-glycol (PEG) modification of particles is necessary to enclose US imaging gas stably and to prepare the

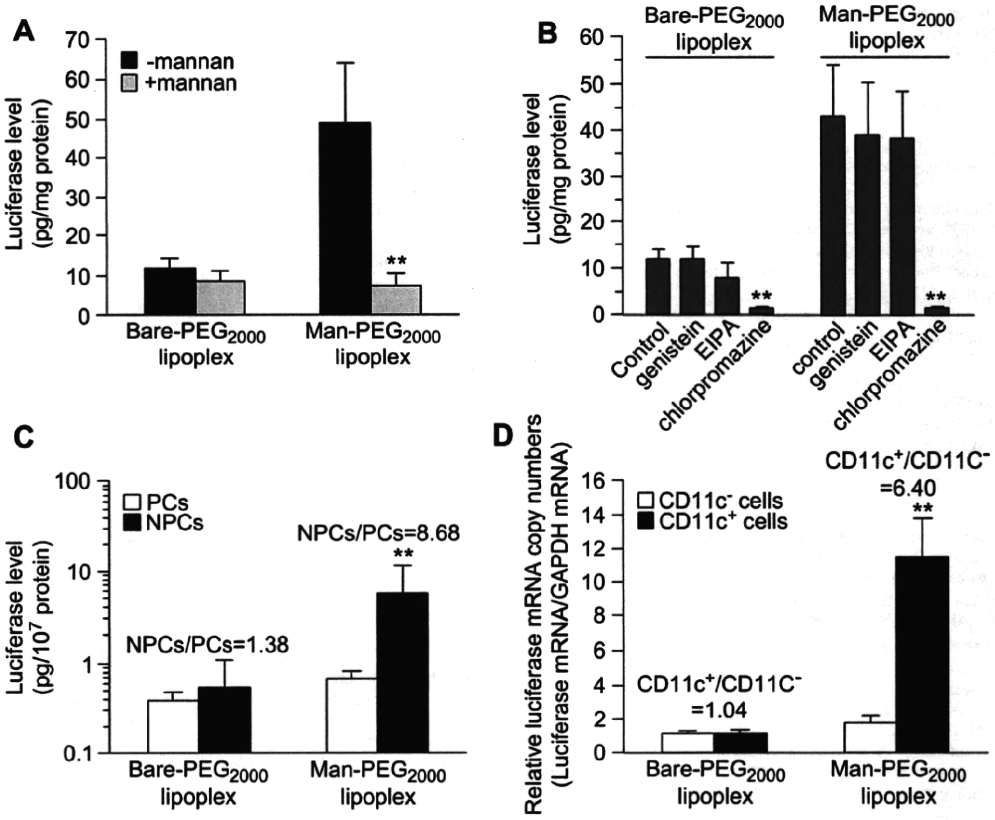

Fig. 2. The mannose receptor-expressing cell-selective gene expression by Man-PEG_{2000} lipoplexes containing Man-PEG_{2000} lipids in vitro and vivo. (A) The level of luciferase expression obtained by Bare-PEG_{2000} lipoplexes and Man-PEG_{2000} lipoplexes (5 μg pDNA) in the absence or presence of 1 mg/mL mannan in mouse cultured macrophages at 24 h after transfection. $^{**}p < 0.01$, compared with the corresponding group of mannan. (B) Inhibition of luciferase expression obtained by Bare-PEG_{2000} lipoplexes and Man-PEG_{2000} lipoplexes (5 μg pDNA) in addition of various endocytosis inhibitors in mouse cultured macrophages at 24 h after transfection. $^{**}p < 0.01$, compared with the corresponding group of control. (C) The level of luciferase expression in mouse hepatic PCs and NPCs after intravenous administration of Bare-PEG_{2000} lipoplexes and Man-PEG_{2000} lipoplexes (50 μg pDNA) in mice at 6 h after transfection. $^{**}p < 0.01$, compared with the corresponding group of PCs. (D) The level of luciferase mRNA expression in mouse splenic $CD11c^+$ cells and $CD11c^-$ cells after intravenous administration of Bare-PEG_{2000} lipoplexes and Man-PEG_{2000} lipoplexes (50 μg pDNA) in mice at 6 h after transfection. $^{**}p < 0.01$, compared with the corresponding group of $CD11c^-$ cells. Each value represents the mean + SD ($n = 3–4$).

small-sized microbubbles for in-vivo administration [12]. Firstly, we developed mannose-conjugated PEG_{2000}-modified lipids (Man-PEG_{2000}-DSPE (Fig. 1)) to prepare the APC-targeted small-sized microbubbles and determined the in-vitro and in-vivo transfection characteristics of mannose-conjugated PEG_{2000}-modified lipoplexes (Man-PEG_{2000} lipoplexes) containing Man-PEG_{2000} lipids. The particle sizes and zeta potentials of Man-PEG_{2000} lipoplexes and non-modified PEG_{2000}-lipoplexes (Bare-PEG_{2000} lipoplexes) were approximately 150 nm and +40 mV, respectively (Supplementary Table 1). In mouse cultured macrophages expressing mannose receptors abundantly, the level of gene expression obtained by Man-PEG_{2000} lipoplexes were significantly higher than those by Bare-PEG_{2000} lipoplexes (Fig. 2A and B). Then, the level of gene expression obtained by Man-PEG_{2000} lipoplexes was suppressed to same extent as that by Bare-PEG_{2000} lipoplexes in the presence of an excess of mannan (Fig. 2A). Moreover, this level of gene expression obtained by Man-PEG_{2000} lipoplexes was also suppressed to same extent as that by Bare-PEG_{2000} lipoplexes in the presence of chlorpromazine (Fig. 2B), which is the inhibitor of clathrin-mediated endocytosis [22]. These results agreed with the results of cellular association of pDNA (Supplementary Fig. 1), and suggest that Man-PEG_{2000} lipoplexes are taken up into the cells via clathrin-mediated endocytosis following the interaction with mannose receptors.

3.2. In-vivo gene transfection properties by Man-PEG_{2000} lipoplexes

Since the degradation of pDNA by nuclease in the blood is one of the critical factors in the in-vivo gene transfection by intravenously administration of lipoplexes, we investigated the stability of Bare-PEG_{2000} lipoplexes and Man-PEG_{2000} lipoplexes against nucleases. Following electrophoresis of naked pDNA and lipoplexes after incubation with DNase I, although naked pDNA underwent the degradation by DNase I, lipoplexes did not undergo the degradation and retained the complex forms (Supplementary Fig. 2). Then, we investigated the gene expression characteristics of Man-PEG_{2000} lipoplexes in the liver and spleen, which are the targeted organs of mannose-modified carriers [27]. In this study, liver was separated in the parenchymal cells (PCs) and non-parenchymal cells (NPCs), and spleen was separated in the dendritic cells ($CD11c^+$ cells) and other cells ($CD11c^-$ cells). As shown in Fig. 2C and D, following intravenous administration of Man-PEG_{2000} lipoplexes, selective gene expression was observed in the hepatic NPCs and the splenic $CD11c^+$ cells, which are the APCs expressing mannose receptors abundantly [28–30].

3.3. In-vitro gene transfection efficiency by Man-PEG_{2000} bubble lipoplexes and US exposure

Although Man-lipoplexes showed the APC-selective gene transfection properties in vivo, this level of gene expression was

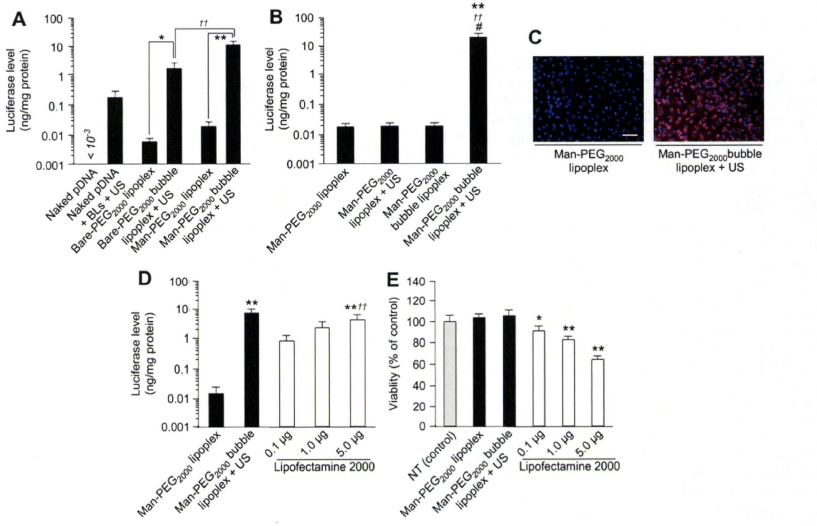

Fig. 3. Enhancement of gene expression by Man-PEG_{2000} bubble lipoplexes and US exposure in vitro. (A) The level of luciferase expression obtained by naked pDNA, naked pDNA + BLs with US exposure, Bare-PEG_{2000} lipoplexes, Bare-PEG_{2000} bubble lipoplexes with US exposure, Man-PEG_{2000} lipoplexes and Man-PEG_{2000} bubble lipoplexes with US exposure (5 μg pDNA) at 24 h after transfection. Significant difference; $^*p < 0.05$; **, $^{\dagger\dagger}p < 0.01$. (B) The level of luciferase expression obtained by Man-PEG_{2000} lipoplexes and Man-PEG_{2000} bubble lipoplexes with or without US exposure (5 μg pDNA) at 24 h after transfection. $^{**}p < 0.01$, compared with Man-PEG_{2000} lipoplex, $^{\dagger\dagger}p < 0.01$, compared with Man-$PEG_{2000}$ lipoplex + US, $^{\#\#}p < 0.01$, compared with Man-PEG_{2000} bubble lipoplex. (C) Representative fluorescent images of cellular association of pDNA obtained by Man-PEG_{2000} lipoplexes and Man-PEG_{2000} bubble lipoplexes with US exposure (5 μg pDNA) at 2 h after treatment. Lipoplexes were constructed with TM-rhodamine-labeled pDNA. TM-rhodamine-labeled pDNA (red), nuclei counterstained by DAPI (blue). Scale bars, 100 μm. (D) Comparison of the level of luciferase expression obtained by Man-PEG_{2000} bubble lipoplexes (5 μg pDNA) and US exposure with that by Lipofectamine 2000. $^{**}p < 0.01$, compared with Man-PEG_{2000} lipoplexes, $^{\dagger\dagger}p < 0.01$, compared with Lipofectamine 2000 (0.1 μg). (E) Comparison of cell viability by transfection using Man-PEG_{2000} bubble lipoplexes (5 μg pDNA) and US exposure with that by Lipofectamine 2000. N.T., non-treatment. $^*p < 0.05$; $^{**}p < 0.01$, compared with N.T. Each value represents the mean + SD ($n = 4$).

low compared with our previous reports [1,19,25]. To enhance the level of gene expression by sonoporation method, we developed Man-PEG_{2000} bubble lipoplexes (Fig. 1) by enclosing US imaging gas (perfluoropropane gas) into Man-PEG_{2000} lipoplexes. The lipid composition of lipoplexes is important for the stable enclosure of US imaging gas. Following optimization of lipid composition, lipoplexes constructed with the saturated lipids only, which have a high melting temperature (T_m), were enclosed US imaging gas stably (Supplementary Table 2). Following enclosure of US imaging gas in lipoplexes, lipoplexes became cloudy and their particle sizes were increased (from 150 nm to 550 nm, approximately) (Supplementary Fig. 3A and Table 3). Then, since the zeta potentials of bubble lipoplexes were lower than that of bubble liposomes and same as that of lipoplexes (Supplementary Tables 1 and 3), it is considered that pDNA is attached on the surface of bubble liposomes. Moreover, the stability against nucleases observed in Man-PEG_{2000} lipoplexes (Supplementary Fig. 2) was maintained after enclosure of US imaging gas into lipoplexes (Supplementary Fig. 3B).

The level of gene expression obtained by Man-PEG_{2000} bubble lipoplexes and US exposure was 500-fold higher than that by Man-PEG_{2000} lipoplexes in mouse cultured macrophages expressing mannose receptors abundantly, and also higher than that by non-modified bubble lipoplexes (Bare-PEG_{2000} bubble lipoplexes, Fig. 1) and US exposure or conventional sonoporation method using naked pDNA and BLs (Fig. 3A). This enhanced gene expression was observed when bubble lipoplexes and US exposure were used for in-vitro gene transfer (Fig. 3B). The cellular association of pDNA obtained by transfection using Man-PEG_{2000} bubble lipoplexes and US exposure was also 10-fold higher than that by Man-PEG_{2000} lipoplexes, and also higher than that by Bare-PEG_{2000} bubble lipoplexes and US exposure or conventional sonoporation method using naked pDNA and BLs (Fig. 3C and Supplementary Fig. 4A). Moreover, this level of gene expression obtained by Man-PEG_{2000} bubble lipoplexes and US exposure was comparable to that by Lipofectamine® 2000, which is widely used as a gene transfection reagent (Fig. 3D). On the other hand, the cytotoxicity by Man-PEG_{2000} bubble lipoplexes and US exposure was lower than that by Lipofectamine® 2000 (Fig. 3E).

3.4. Intracellular uptake properties of pDNA by Man-PEG_{2000} bubble lipoplexes and US exposure

The gene expression obtained by Man-PEG_{2000} bubble lipoplexes and US exposure was significantly suppressed in the presence of an excess of mannan (Fig. 4A). Therefore, the interaction with mannose receptors on the cell membrane is involved in the gene transfection by Man-PEG_{2000} bubble lipoplexes and US exposure, similar to the gene transfection by Man-PEG_{2000} lipoplexes. On the other hand, unlike Man-PEG_{2000} lipoplexes (Fig. 2B), the gene expression obtained by Man-PEG_{2000} bubble lipoplexes and US exposure was not suppressed in the presence of chlorpromazine (Fig. 4B), which is a clathrin-mediated endocytosis inhibitor [22]. These results agreed with the results of cellular association of pDNA (Supplementary Fig. 4B), and indicated that pDNA delivered by Man-PEG_{2000} bubble lipoplexes was directly introduced into the cytoplasm without mediating endocytosis by the gene transfection using Man-PEG_{2000} bubble lipoplexes and US exposure.

3.5. In-vivo gene transfection efficiency by Man-PEG_{2000} bubble lipoplexes and US exposure

As shown in Fig. 5A and B, the level of gene expression obtained by Man-PEG_{2000} bubble lipoplexes and US exposure was

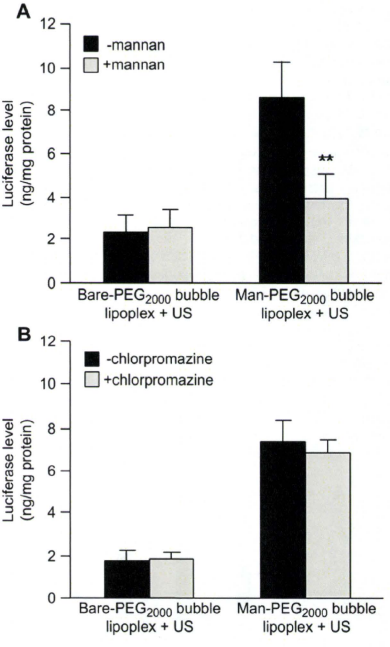

Fig. 4. Effects of mannan and chlorpromazine on gene expression by Man-PEG_{2000} bubble lipoplexes and US exposure in vitro. (A) The level of luciferase expression obtained by Bare-PEG_{2000} bubble lipoplexes with US exposure and Man-PEG_{2000} bubble lipoplexes with US exposure (5 μg pDNA) in the absence or presence of 1 mg/mL mannan at 24 h after transfection. $^{**}p < 0.01$, compared with the corresponding group of mannan. (B) The level of luciferase expression by Bare-PEG_{2000} bubble lipoplexes with US exposure and Man-PEG_{2000} bubble lipoplexes with US exposure (5 μg pDNA) in the absence or presence of 50 μM chlorpromazine at 24 h after transfection. Each value represents the mean + SD ($n = 4$).

500 ~ 800-fold higher than that by Man-PEG_{2000} lipoplexes, and also higher than that by Bare-PEG_{2000} bubble lipoplexes and US exposure or the conventional sonoporation method using naked pDNA and BLs in the liver and spleen, which are the targeted organs of mannose-modified carriers [27]. This enhanced gene expression in the liver and spleen was observed when bubble lipoplexes and US exposure were used for in-vivo gene transfer (Fig. 5C and D). Moreover, this gene expression obtained by Bare-PEG_{2000} bubble lipoplexes with US exposure or Man-PEG_{2000} bubble lipoplexes with US exposure in the liver and spleen remained higher than that by Bare-PEG_{2000} lipoplexes or Man-PEG_{2000} lipoplexes for at least 48 h, respectively (Fig. 5E and F). In addition, the gene expression was also enhanced in the US-exposed organ specifically following gene transfection by direct US exposure to the targeted organ after intravenous administration of Man-PEG_{2000} bubble lipoplexes (Supplementary Fig. 5). On the other hand, the increase of gene expression by bubble lipoplexes and US exposure was not observed in other organ such as lung, kidney and heart (Fig. 5G and H).

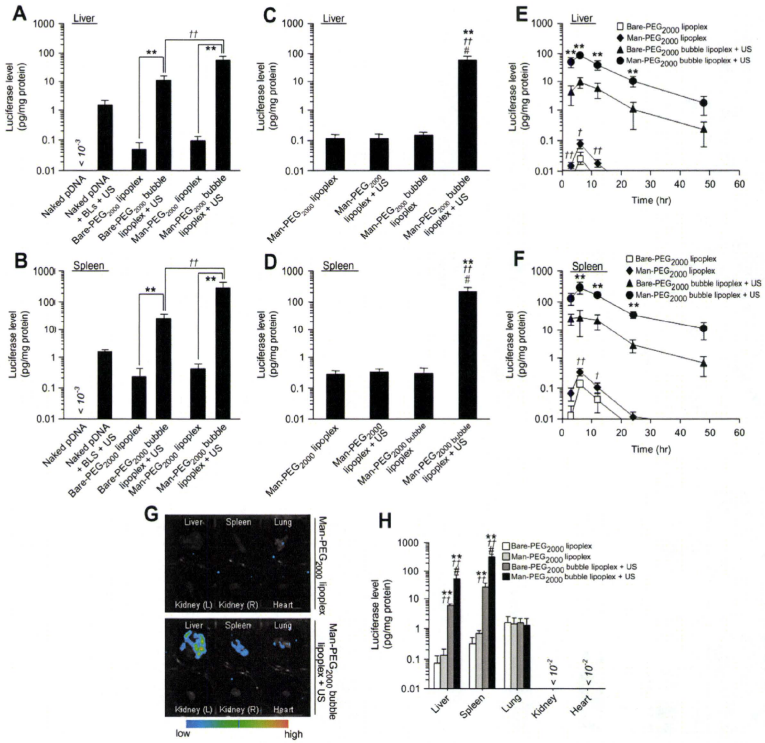

Fig. 5. Enhancement of mannose receptor-expressing cells-selective gene expression by Man-PEG_{2000} bubble lipoplexes and US exposure in vivo. (A, B) The level of luciferase expression obtained by naked pDNA, naked pDNA + BLs with US exposure, Bare-PEG_{2000} lipoplexes, Bare-PEG_{2000} bubble lipoplexes with US exposure, Man-PEG_{2000} lipoplexes and Man-PEG_{2000} bubble lipoplexes with US exposure (50 μg pDNA) in the liver (A) and spleen (B) at 6 h after transfection. Significant difference; **, $^{\dagger\dagger}p < 0.01$. (C, D) The level of luciferase expression obtained by Man-PEG_{2000} lipoplexes and Man-PEG_{2000} bubble lipoplexes with or without US exposure (50 μg pDNA) in the liver (C) and spleen (D) at 6 h after transfection. $^{**}p < 0.01$, compared with Man-PEG_{2000} lipoplex, $^{\dagger\dagger}p < 0.01$, compared with Man-$PEG_{2000}$ lipoplex + US, $^{\#\#}p < 0.01$, compared with Man-PEG_{2000} bubble lipoplex. (E, F) Time-course of luciferase expression in the liver (E) and spleen (F) after transfection by Bare-PEG_{2000} lipoplexes, Man-PEG_{2000} lipoplexes, Bare-PEG_{2000} bubble lipoplexes with US exposure and Man-PEG_{2000} bubble lipoplexes with US exposure (50 μg pDNA). Each value represents the mean ± SD ($n = 4$). $^{**}p < 0.01$, compared with Bare-PEG_{2000} bubble lipoplex + US, $^{\dagger}p < 0.05$; $^{\dagger\dagger}p < 0.01$, compared with Bare-$PEG_{2000}$ lipoplex. (G) In-vivo imaging photographs of luciferase expression in the isolated organs at 6 h after transfection by Man-PEG_{2000} lipoplexes and Man-PEG_{2000} bubble lipoplexes with US exposure (50 μg pDNA). (H) The level of luciferase expression in each organ at 6 h after transfection by Bare-PEG_{2000} lipoplexes, Man-PEG_{2000} lipoplexes, Bare-PEG_{2000} bubble lipoplexes with US exposure and Man-PEG_{2000} bubble lipoplexes with US exposure (50 μg pDNA). $^{**}p < 0.01$, compared with the corresponding group of Bare-PEG_{2000} lipoplex, $^{\dagger\dagger}p < 0.01$, compared with the corresponding group of Man-PEG_{2000} lipoplex. $^{\#\#}p < 0.01$, compared with the corresponding group of Bare-PEG_{2000} bubble lipoplex + US. Each value represents the mean + SD ($n = 4$).

3.6. Targeted cell-selective gene transfection properties by Man-PEG_{2000} bubble lipoplexes and US exposure in vivo

We investigated the mannose receptor-expressing cell selectivity of gene expression by transfection using Man-PEG_{2000} bubble lipoplexes and US exposure. In the liver, the level of gene expression in the hepatic NPCs expressing mannose receptors was significantly higher than that in the hepatic PCs following gene transfection by Man-PEG_{2000} bubble lipoplexes and US exposure (Fig. 6A). This difference in gene expression between the NPCs and PCs obtained by Man-PEG_{2000} bubble lipoplexes and US exposure was similar to that by Man-PEG_{2000} lipoplexes, although the level of gene expression in the NPCs and PCs was markedly higher. On the other hand, selective gene expression in the NPCs was not observed by Bare-PEG_{2000} bubble lipoplexes and US exposure.

In the spleen, the level of mRNA expression in the $CD11c^+$ cells, which are the splenic dendritic cells expressing mannose receptors, was significantly higher than that in the $CD11c^-$ cells following transfection by Man-PEG_{2000} bubble lipoplexes and US exposure (Fig. 6B). On the other hand, selective gene expression in the $CD11c^+$ cells was not observed by Bare-PEG_{2000} bubble lipoplexes and US exposure.

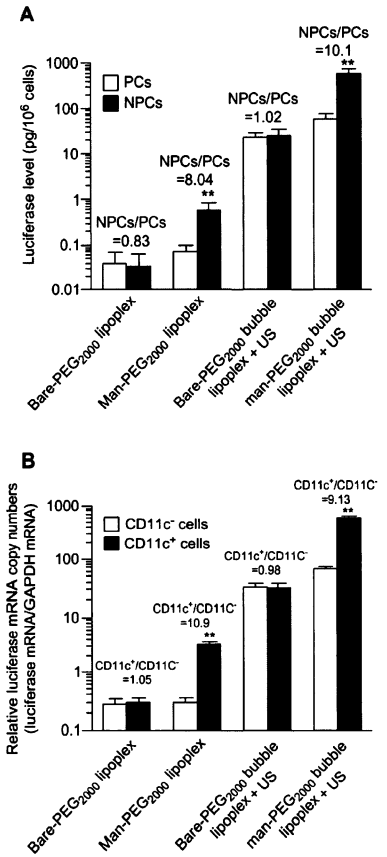

Fig. 6. Hepatic and splenic cellular localization of luciferase expression by Man-PEG_{2000} bubble lipoplexes and US exposure. (A) Hepatic cellular localization of luciferase expression at 6 h after transfection by Bare-PEG_{2000} lipoplexes, Man-PEG_{2000} lipoplexes, Bare-PEG_{2000} bubble lipoplexes with US exposure and Man-PEG_{2000} bubble lipoplexes with US exposure (50 μg pDNA). $^{**}p < 0.01$, compared with the corresponding group of PCs. (B) Splenic cellular localization of luciferase mRNA expression at 6 h after transfection by Bare-PEG_{2000} lipoplexes, Man-PEG_{2000} lipoplexes, Bare-PEG_{2000} bubble lipoplexes with US exposure and Man-PEG_{2000} bubble lipoplexes with US exposure (50 μg pDNA). $^{**}p < 0.01$, compared with the corresponding group of $CD11c^-$ cells. Each value represents the mean + SD ($n = 4$).

3.7. In-vivo distribution properties of pDNA by Man-PEG_{2000} bubble lipoplexes and US exposure

Next, to elucidate the mechanism of enhanced in-vivo gene expression using Man-PEG_{2000} bubble lipoplexes and US exposure, we investigated the effect on the tissue distribution of pDNA followed by gene transfection. In this study, Bare-PEG_{2000} bubble lipoplexes and Man-PEG_{2000} bubble lipoplexes constructed with radio-labeled pDNA were intravenously administrated, and then mice were subjected to external US exposure. As shown in Fig. 7, in the case of both bubble lipoplexes, the retention time of pDNA in the blood was slightly reduced and the distribution of pDNA delivered by bubble lipoplexes was significantly increased by US exposure in the liver and spleen (Fig. 7). Moreover, the amount of pDNA distributed in the liver and spleen by Man-PEG_{2000} bubble lipoplexes and US exposure (Fig. 7A) was higher than that by Bare-PEG_{2000} bubble lipoplexes and US exposure (Fig. 7B). On the other hand, no increase of pDNA distribution followed by US exposure was observed in the lung.

3.8. The liver toxicity by Man-PEG_{2000} bubble lipoplexes and US exposure

We examined ALT and AST activities in the serum to investigate the liver toxicity by gene transfection using Man-PEG_{2000} bubble lipoplexes and US exposure. ALT and AST activities in the serum were increased by gene transfection using Bare-PEG_{2000} lipoplexes and Man-PEG_{2000} lipoplexes. On the other hands, the increase of ALT and AST activities was not observed by gene transfection using Bare-PEG_{2000} bubble lipoplexes and Man-PEG_{2000} bubble lipoplexes with US exposure (Fig. 8).

3.9. Antigen presentation on MHC class I molecules in immunized splenic dendritic cells

To investigate the DNA vaccine effects by Man-PEG_{2000} bubble lipoplexes and US exposure, we prepared Man-PEG_{2000} bubble lipoplexes constructed with pDNA expressing OVA as a model antigen. Firstly, to investigate the antigen (OVA) presentation on MHC class I molecules in the splenic dendritic cells ($CD11c^+$ cells) by Man-PEG_{2000} bubble lipoplexes constructed with pCMV-OVA and US exposure, the splenic $CD11c^+$ cells isolated from once-immunized mice were co-incubated with CD8-OVA1.3 cells, which are T cell hybridomas with specificity for OVA. Following measurement of IL-2 to evaluate the activation of T cells, the IL-2 secretion from activated CD8-OVA1.3 cells co-incubated with the $CD11c^+$ cells isolated from mice immunized by Man-PEG_{2000} bubble lipoplexes and US exposure was the highest of all (Fig. 9A). This result indicates that DNA vaccination by Man-PEG_{2000} bubble lipoplexes constructed with pCMV-OVA and US exposure can induce significantly high $CD8^+$-T lymphocyte activation.

3.10. Antigen-specific cytokine secretion from immunized splenic cells

We evaluated the OVA-specific cytokine secretion from the splenic cells immunized by Man-PEG_{2000} bubble lipoplexes constructed with pCMV-OVA and US exposure. Following optimization of immunization schedule, it was shown that a 2 week interval was necessary to achieve the same level of gene expression as former transfection in the spleen (Supplementary Fig. 6) and at least three times immunization was necessary to effective anti-tumor effects by DNA vaccination using this method (Supplementary Fig. 7). Therefore, the immunization to mice was performed according to the protocol shown in Fig. 9B. As shown in Fig. 9C, in the presence of OVA, the highest amount of IFN-γ (Th1 cytokine) was secreted from splenic cells harvested from mice immunized with Man-PEG_{2000} bubble lipoplexes and US exposure. On the other hand, no secretion of IFN-γ was observed in any of the groups in the absence of OVA. Moreover, the secretion of IL-4 (Th2 cytokine) was not increased in any of the groups both in the presence or absence of OVA (Fig. 9C). These results suggest that immunization by Man-PEG_{2000} bubble lipoplexes constructed with